

Test of a modified BCS theory performance in the Picket Fence Model

V.Yu. Ponomarev ^{a,*}, A.I. Vdovin ^b

^a *Institut für Kernphysik, Technische Universität Darmstadt, D-64289 Darmstadt, Germany*

^b *Bogoliubov Laboratory of Theoretical Physics, Joint Institute for Nuclear Research, 141980 Dubna, Russia*

Received 1 February 2008; received in revised form 27 February 2009; accepted 3 March 2009

Available online 6 March 2009

Abstract

Analyses of a modified BCS (MBCS) theory performance at finite temperatures in the Picket Fence Model (PFM) for light and heavy systems are presented. Both symmetric, $\Omega = N$ (N particles on Ω doubly-degenerate levels), and asymmetric, $\Omega \neq N$, versions of the PFM are considered. Quantities determined exactly from particle–hole symmetry of the symmetric PFM are calculated in the MBCS. They are found in significant deviation from the exact values starting from far below the critical temperatures of the conventional BCS. Consequences of the MBCS prediction that heating generates a thermal constituent of the pairing gap, are discussed. The question of thermodynamical consistency of the MBCS is also addressed.

© 2009 Elsevier B.V. All rights reserved.

PACS: 21.60.-n; 24.10.Pa; 24.60.-k; 24.60.Ky

Keywords: BCS theory; Finite temperature; Phase transition

1. Introduction

A modified BCS (MBCS) theory for treating pairing correlations in atomic nuclei at finite temperatures [1,2] has been recently tested [3] in the Picket Fence Model (PFM) in which N particles are distributed over Ω doubly-degenerate levels. The PFM with $N = \Omega$ is usually considered in the literature.

* Corresponding author.

E-mail address: ponomare@crunch.ikp.physik.tu-darmstadt.de (V.Yu. Ponomarev).

The MBCS predicts a smooth decreasing behavior for a pairing gap as temperature T increases up to some T_M when the theory suddenly breaks down. It was reported [3,4] that adding one extra level ($\Omega = N + 1$) extends the MBCS applicability to much higher temperatures. Studies of the model in Ref. [5] notified that the exceptional behavior of the MBCS pairing gap is limited to the $\Omega = N + 1$ case only. Here we provide a more systematic study for $\Omega \neq N$ examples in the PFM. This is done in Section 3.

In Section 4, we address the key question of the article: what is the range of temperatures where the MBCS provides a reasonable description. For that, we examine some quantities which are known exactly in the $N = \Omega$ PFM because of symmetry. In Section 5, the MBCS prediction that not only the pairing force but also the heating itself generates the pairing gap, is discussed. In Section 6 we investigate the thermodynamical consistency of the MBCS.

2. Introduction to the MBCS approach

In the MBCS treatment of the pairing problem at finite temperature, in addition to the canonical Bogoliubov transformation from particle creation a_{jm}^\dagger and annihilation a_{jm} operators to quasiparticle operators $\{\alpha_{jm}^\dagger, \alpha_{jm}\}$:

$$\begin{aligned}\alpha_{jm}^\dagger &= u_j a_{jm}^\dagger - v_j a_{j\bar{m}}, \\ \alpha_{j\bar{m}} &= u_j a_{j\bar{m}} + v_j a_{jm}^\dagger,\end{aligned}\tag{1}$$

a secondary temperature-dependent Bogoliubov transformation to new bar-quasiparticles $\{\bar{\alpha}_{jm}^\dagger, \bar{\alpha}_{jm}\}$:

$$\begin{aligned}\bar{\alpha}_{jm}^\dagger &= \sqrt{1 - n_j} \alpha_{jm}^\dagger + \sqrt{n_j} \alpha_{j\bar{m}}, \\ \bar{\alpha}_{j\bar{m}} &= \sqrt{1 - n_j} \alpha_{j\bar{m}} - \sqrt{n_j} \alpha_{jm}^\dagger\end{aligned}\tag{2}$$

and a new ground state $|\bar{0}\rangle$, a vacuum for the bar-quasiparticles, are introduced. The index jm corresponds to the level of a spherically symmetric mean field with quantum numbers $j \equiv [n, l, j]$, projection m , and energy ε_j . Tilde in Eqs. (1), (2) and below means time reversal operation: $\alpha_{j\bar{m}} = (-1)^{j-m} \alpha_{j-m}$. Thermal quasiparticle occupation numbers $n_j = 1/(1 + \exp(E_j/T))$ are functions of a quasiparticle energy E_j and temperature T .

Combining transformations (1) and (2) one obtains Bogoliubov transformation from particle to bar-quasiparticle operators:

$$\begin{aligned}\bar{\alpha}_{jm}^\dagger &= \bar{u}_j a_{jm}^\dagger - \bar{v}_j a_{j\bar{m}}, \\ \bar{\alpha}_{j\bar{m}} &= \bar{u}_j a_{j\bar{m}} + \bar{v}_j a_{jm}^\dagger\end{aligned}\tag{3}$$

where

$$\begin{aligned}\bar{u}_j &= u_j \sqrt{1 - n_j} + v_j \sqrt{n_j}, \\ \bar{v}_j &= v_j \sqrt{1 - n_j} - u_j \sqrt{n_j}.\end{aligned}\tag{4}$$

Minimization of the pairing Hamiltonian cannot depend on whether coefficients of the unitary transformation are written with bar in Eq. (3) or without it in Eq. (1). Accordingly, applying Eq. (3) one should obtain the same equations and solutions as in the BCS($T = 0$) theory (which uses Eq. (1)) but in bar-variables. They are the pairing gap equations:

$$\begin{aligned}
 N &= 2 \sum_j (j + 1/2) \bar{v}_j^2, \\
 \bar{\Delta} &= G \sum_j (j + 1/2) \bar{u}_j \bar{v}_j
 \end{aligned} \tag{5}$$

solving which one determines a Fermi surface energy \bar{E}_F and a pairing gap $\bar{\Delta}$, and analytical expressions for eigen-energies:

$$\bar{E}_j = \sqrt{(\varepsilon_j - \bar{E}_F)^2 + \bar{\Delta}^2} \tag{6}$$

and eigen-vectors:

$$\begin{aligned}
 \bar{u}_j &= \sqrt{\frac{1}{2} \left(1 + \frac{\varepsilon_j - \bar{E}_F}{\bar{E}_j} \right)}, \\
 \bar{v}_j &= \sqrt{\frac{1}{2} \left(1 - \frac{\varepsilon_j - \bar{E}_F}{\bar{E}_j} \right)}.
 \end{aligned} \tag{7}$$

The MBCS founders suggest to solve Eqs. (5) for obtaining \bar{E}_F and $\bar{\Delta}$ but at the same time to associate expressions (6), (7) with $\alpha_{jm}^\dagger |0\rangle$ states instead of the MBCS eigen-states $\bar{\alpha}_{jm}^\dagger |\bar{0}\rangle$, i.e. to use

$$E_j = \sqrt{(\varepsilon_j - \bar{E}_F)^2 + \bar{\Delta}^2} \tag{8}$$

and

$$\begin{aligned}
 u_j &= \sqrt{\frac{1}{2} \left(1 + \frac{\varepsilon_j - \bar{E}_F}{E_j} \right)}, \\
 v_j &= \sqrt{\frac{1}{2} \left(1 - \frac{\varepsilon_j - \bar{E}_F}{E_j} \right)}
 \end{aligned} \tag{9}$$

as in the conventional BCS. Coefficients $\{\bar{u}_j, \bar{v}_j\}$ are calculated from Eq. (4). Eqs. (4), (5), (8), (9) form the complete set of the MBCS equations.¹ It is essential to keep in mind that this set of the MBCS equations was not obtained analytically (as, e.g., the BCS equations). It was written down in analogy to the BCS equations as far as the pairing Hamiltonian in terms of bar- and Bogoliubov quasiparticles look formally the same. Inconsistency in this analogy is that solutions of the eigen-problem for the pairing Hamiltonian are attributed to non-eigen-states $\alpha_{jm}^\dagger |0\rangle$ in the MBCS.

Expressions for physical observables (like the system energy, etc.) are obtained in the MBCS by formal replacement of the $\{u_j, v_j\}$ coefficients in corresponding BCS($T = 0$) expressions by the $\{\bar{u}_j, \bar{v}_j\}$ coefficients.

3. MBCS pairing gap in PFM systems with $\Omega = N$ and $\Omega \neq N$

The PFM or Richardson model is widely used as a test model for the pairing problem. It is the pairing Hamiltonian applied to a system of N fermions distributed over Ω equidistant levels. All

¹ Bar on top of \bar{E}_F and $\bar{\Delta}$ is omitted below.

levels are doubly degenerate for spin up and down. The levels below (above) the Fermi surface will be referred to as holes (particles) and labeled by “ $-i$ ” (“ i ”). Their single particle energies are $\varepsilon_{-i} = (0.5 - i)$ MeV for holes and $\varepsilon_i = (-0.5 + i)$ MeV for particles, where $i = 1, 2, \dots$ (i.e. $\varepsilon_i = -\varepsilon_{-i}$). In all calculations presented below (except for the ones in Fig. 5(c), (d) and Fig. 7(a), the pairing strength parameter G is adjusted so that the pairing gap Δ equals 1 MeV at zero temperature.

When the number of particles N in the PFM is not big, the pairing Hamiltonian can be diagonalized exactly. Comparison in [6] of particle occupation numbers and specific heat in MBCS predictions to the same quantities obtained from an exact solution for the $N = \Omega = 10$ system reveal substantial deviations. It has been argued [3,4] that the cause of deviations is a limited number of levels in the system. Below, we compare MBCS predictions to exact results which do not require the Hamiltonian diagonalization but based on internal particle–hole symmetry of the PFM with $N = \Omega$ (to be referred to as the conventional PFM). Due to this symmetry, at any temperature and for any number of particles N :

(a) the energy of the Fermi surface E_F equals exactly 0 MeV:

$$E_F \equiv 0; \tag{10}$$

(b) the quasiparticle energies E_i for particles and holes should be degenerate:

$$E_i = \sqrt{(\varepsilon_i - E_F)^2 + \Delta^2} \equiv \sqrt{(\varepsilon_{-i} - E_F)^2 + \Delta^2} = E_{-i} \tag{11}$$

because of (10);

(c) the particle occupation probabilities (Bogoliubov u_i and v_i coefficients) are related as:

$$u_i = \sqrt{\frac{1}{2} \left(1 + \frac{\varepsilon_i - E_F}{E_i} \right)} \equiv \sqrt{\frac{1}{2} \left(1 - \frac{\varepsilon_{-i} - E_F}{E_{-i}} \right)} = v_{-i} \tag{12}$$

because of (10), (11);

(d) the thermal quasiparticle occupation numbers n_i and quasiparticle-number fluctuations $\delta N_i = \sqrt{n_i(1 - n_i)}$ should be equal for particles and holes with the same i :

$$n_i \equiv n_{-i} \quad \text{and} \quad \delta N_i \equiv \delta N_{-i} \tag{13}$$

because of (11).

Of course, an asymmetric version of the PFM with $\Omega = N + k$ (where $k = -N/2 + 1, \dots, -1, 1, \dots, \infty$) may be considered as well but Eqs. (10)–(13) are not valid for it.

The first test of the MBCS performance in the conventional PFM with $N = \Omega = 10$ revealed that at $T \approx 1.75$ MeV the system undertakes a phase transition which manifests itself as a sharp simultaneous increase in the pairing gap, a sharp decrease of the system energy and a discontinuity in the specific heat C_V (this phase transition was defined in [6] as a superfluid – super-superfluid phase transition). This critical temperature was denoted as T_M in Refs. [3,4]. It was found that T_M linearly increases with the number of particles N in the conventional PFM. It was also reported that enlarging the space by one more level, $\Omega = N + 1$, restores the MBCS applicability to much higher temperatures even for $N \leq 14$ systems [3,4].

Fig. 1 plots the MBCS pairing gap for $N = 14$ particles and $\Omega = N + k$ levels with k changing from -4 to 50 (solid curves). Indeed, the MBCS gap is small and almost constant above the critical temperature T_c of the conventional BCS when the example of extended configuration space with $k = 1$, is considered. However, when one more extra level is added to the PFM

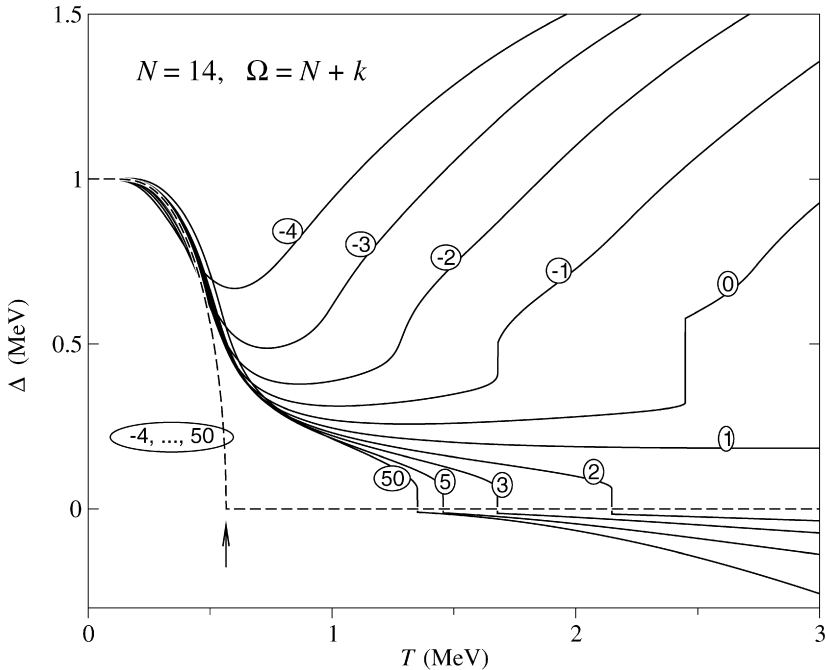


Fig. 1. MBCS pairing gap Δ for the system of $N = 14$ particles on $\Omega = N + k$ levels (solid curves). The BCS pairing gap is plotted by the dashed curve. The k values are indicated in an oval at each curve. The conventional critical temperature T_C is shown by the vertical arrow.

($k = 2$) the MBCS pairing gap sharply drops to negative value at $T_M = 2.15$ MeV and its absolute value starts to grow as a function of T . With an additional enlarging of the configuration space ($k = 3, 4, \dots$), the MBCS pairing gap behavior remains similar to $k = 2$ example with T_M becoming smaller as k increases. On the other side, in the case of the conventional PFM ($k = 0$) and reduced configuration space ($k = -1, -2, \dots$), the MBCS gap starts to grow above some T_M which becomes again smaller as $|k|$ increases.

The pairing gap of the conventional BCS theory is shown in Fig. 1 by the dashed curve for comparison. It is impossible to visually distinguish the results when k value changes from -4 to 50 .

We have performed additional calculations for the asymmetric PFM with N changing from 6 to 100. The results look similar to the ones in Fig. 1. In all these examples, there exists only a single case $k = 1$ with exceptionally large T_M which grows almost linearly with N . For all other k values, the MBCS breaks down at much lower T_M . The critical temperature T_M systematically decreases with increasing of the $|k - 1|$ value.

From the systematic analysis of the MBCS pairing gap behavior in the PFM we conclude that:

- (1) the MBCS predictions are very sensitive to details of the single particle spectrum employed;
- (2) the MBCS predicts two typical scenarios for the system evolution with heating. As temperature increases, the system undertakes either (a) a superfluid – super-superfluid phase transition (examples with $k \leq 0$ in Fig. 1) or (b) a phase transition from a superfluid phase

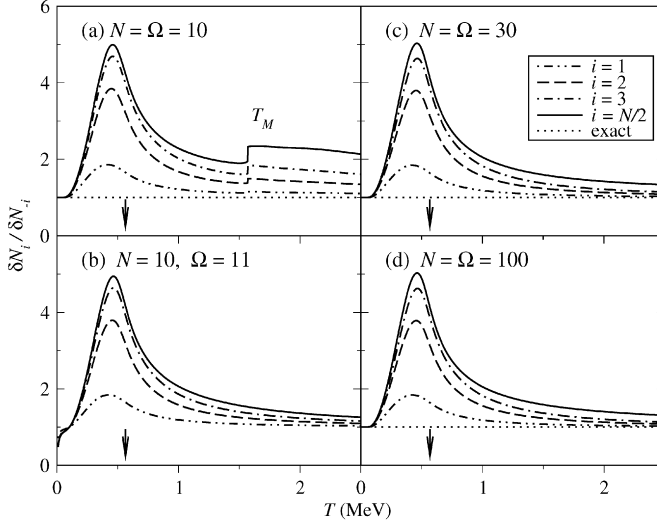


Fig. 2. MBCS predictions for the ratios of quasiparticle-number fluctuations $\delta N_i / \delta N_{-i}$ in different (N, Ω) systems. The exact result $\delta N_i / \delta N_{-i} \equiv 1$ in figures (a), (c), (d) is shown by the dotted line. The conventional critical temperature T_c is shown by the vertical arrow.

with a positive gap to another superfluid phase but with a negative gap² (examples with $k > 1$ in Fig. 1). In both the cases, the MBCS predicts that above some critical temperature the pairing gap $|\Delta|$ starts to grow;

- (3) for each number of particles N , there exists a single exceptional case with the number of PFM levels $\Omega = N + 1$ for which the MBCS mimics the thermal behavior of the average pairing gap in Ref. [7] where the normal – superfluid phase transition is washed out and above T_c the gap remains rather small but positively finite.

4. Applicability of the MBCS at finite temperature

A criterion of the MBCS applicability has been suggested in Refs. [3,4]. According to it, the quasiparticle-number fluctuations δN_i should be symmetric with the respect to the Fermi surface. The conventional PFM with its particle–hole symmetry, see Eqs. (11), (13), is an ideal system to determine the temperature range where the MBCS predictions are most accurate.

Fig. 2 presents the ratios $\delta N_i / \delta N_{-i}$, for different levels i which are plotted by different line-types. The deviation of these ratios from 1 is a measure of the asymmetry in the quasiparticle-number fluctuations which quantifies on the level of violation of the criterion the MBCS applicability. The results are presented for (a) light, $N = 10$, (c) medium, $N = 30$, and (d) heavy, $N = 100$, systems. The exact result, Eq. (13), is given by the dotted line. For comparison, we also provide in Fig. 2(b) an example with $\Omega = N + 1$.

² In the BCS, the gauge is fixed by a convention that u and v coefficients of the canonical Bogoliubov transformation are real and positively defined. It leads to always positive BCS pairing gap. The same convention is used in the MBCS. The pairing gap turning negative in MBCS predictions indicates that some processes play more important role in generating the gap than the pairing force (see below).

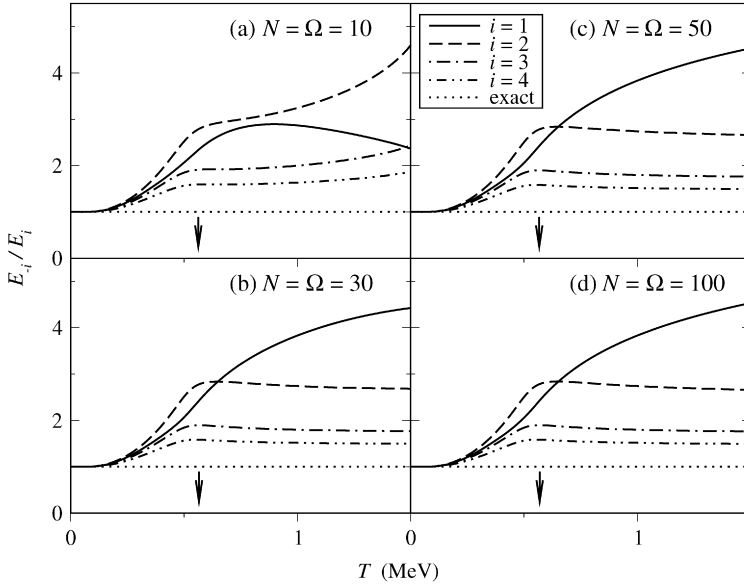


Fig. 3. MBCS predictions for the ratios of quasiparticle energies (E_{-i}/E_i) in different $N = \Omega$ systems. The exact result ($E_{-i}/E_i \equiv 1$) is shown by the dotted line. The conventional critical temperature T_c is shown by the vertical arrow.

The temperature dependence of the ratios $\delta N_i/\delta N_{-i}$ is almost the same for all systems in Fig. 2. The asymmetry in δN_i sets in at $T \approx 100$ keV, it rapidly grows, reaching its maximum in the vicinity of T_c , and then drops down again. A correlation between the magnitude of the deviation and the energy of a particle/hole pair relative to the Fermi surface is observed.

Only the lightest system, $N = 10$, in Fig. 2 reaches the temperature T_M below 2.5 MeV. At this temperature, the asymmetry in δN_i also slightly increases but the effect is very modest compared to what we witness at lower temperatures. Our results in Fig. 2 demonstrate that the criterion of the MBCS applicability in [3,4] does not explain the MBCS breaking down above T_M because it is violated even stronger at lower temperatures where the MBCS pairing gap looks reasonable at first glance.

Let us briefly check how other properties of the conventional PFM, Eqs. (10)–(13), are fulfilled in the MBCS predictions. Since the quantities δN_i and n_i in Eq. (13) are closely related, the behavior of the ratios n_i/n_{-i} is very similar to the one of $\delta N_i/\delta N_{-i}$ in Fig. 2. The strongest deviation of n_i/n_{-i} from 1 takes place near T_c and reaches the value of 25.

The accuracy of the MBCS predictions for the quasiparticle energies, Eq. (11), and for the particle occupation probability, Eq. (12), with $i = 1$ is examined in Fig. 3 and Fig. 4(a), respectively. Fig. 4(b) shows the calculated Fermi surface energy as a function of temperature for different particle numbers. Except for small temperatures ($T \leq 100$ keV) the Fermi surface energy deviates from zero expected from Eq. (10). Furthermore, the results in light and heavy systems are very similar, at least qualitatively. While the accuracy in description of the δN_i and n_i quantities in the MBCS predictions improves at higher temperatures, this is not the case for the quantities in Figs. 3 and 4.

The results in Figs. 2–4 indicate that as soon as heating starts to play a role, the MBCS fails to describe genuine properties of the conventional PFM. Deviations from the exact results are very strong and almost independent of the particle number N .

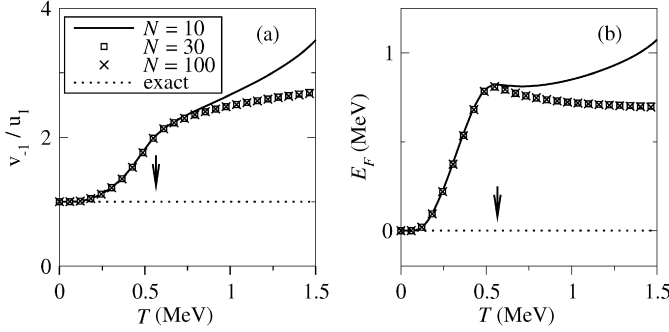


Fig. 4. MBCS predictions for (a) ratios (v_{-1}/u_1) and (b) the energy of the Fermi level E_F in $N = \Omega = 10, 30,$ and 100 systems. The exact results (a) $(v_{-1}/u_1) \equiv 1$ and (b) $E_F \equiv 0$ for these systems are shown by dotted lines. The conventional critical temperature T_c is shown by the vertical arrow.

5. MBCS pairing gap: Quantal and thermal constituents

Since the criterion of the MBCS applicability in Refs. [3,4] is violated much stronger at lower temperature than at T_M and above, an alternative explanation of the breakdown temperature T_M is needed. Below, we analyze the MBCS pairing gap. Substituting (3) into (5), Eq. (5) for the MBCS gap can be rewritten as the sum of two terms $\Delta = \Delta_q + \delta\Delta$. The first of them:

$$\Delta_q = G \sum_j (j + 1/2)(1 - 2n_j)u_j v_j, \tag{14}$$

looks similar to the pairing gap of the conventional BCS and referred in [3] as a quantal part. The second one:

$$\delta\Delta_h = G \sum_j^{\text{holes}} (j + 1/2)(v_j^2 - u_j^2)\sqrt{n_j(1 - n_j)} \quad \text{for holes,} \tag{15}$$

$$\delta\Delta_p = G \sum_j^{\text{part.}} (j + 1/2)(v_j^2 - u_j^2)\sqrt{n_j(1 - n_j)} \quad \text{for particles,} \tag{16}$$

represents an extra thermal part.

Fig. 5 presents the MBCS gap for (a) light and (b) heavy PFM systems by the thick solid curve. The Δ_q part of it is shown by the thin solid curve, it quickly drops to almost zero above T_c . The additional thermal part for holes (particles) is plotted by the dashed (dot-dashed) curve. The quantity $\delta\Delta_h$ is always positive ($v_i > u_i$) and the quantity $\delta\Delta_p$ is always negative ($u_i > v_i$); their absolute values increase with temperature.

In the conventional BCS, pairing is generated by the pairing force. As temperature increases the thermal scattering of nucleons becomes stronger and stronger and finally destroys the pairing at T_c . The MBCS suggests a different picture, where the heating itself generates an extra thermal constituent of the pairing gap: positive for holes and negative for particles. The heavier the system, the stronger a thermal pairing gap may be generated. A similar phenomenon takes place in calculations with realistic single particle spectra (see Fig. 5(c) and (d) where the pairing gap behavior in ^{120}Sn is presented for neutrons and protons, respectively).

In a magic nuclear system the pairing strength is too weak to generate pairing. Nevertheless, the MBCS predicts that the heating should develop the pairing gap at finite T even in such a case

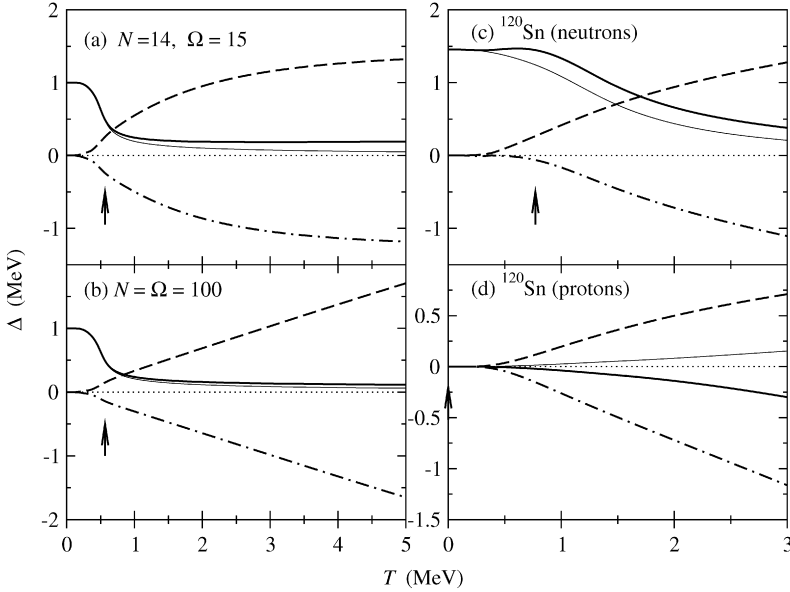


Fig. 5. MBCS pairing gap (thick solid curve) for the PFM systems with (a) $N = 14$, $\Omega = 15$ and (b) $N = \Omega = 100$ and in a calculation with a realistic single particle spectrum for ^{120}Sn : (c) neutron and (d) proton systems. This gap is the sum of a Δ_q , Eq. (14), (particles plus holes – thin solid curve) and extra thermal (holes – dashed curve, particles – dot-dashed curve) parts. The conventional critical temperature T_c is shown by the vertical arrow.

[cf. Eqs. (15)–(16)]. An example of the pairing induced by heating in such a system is shown in Fig. 5(d).

The BCS $T = 0$ solution evolves as temperature increases. Its evolution in the MBCS involves two almost linearly growing functions $\delta\Delta_h$ and $-\delta\Delta_p$ which should cancel each other with a high accuracy in a large temperature interval.³ At T_M the balance between these two terms is broken and the MBCS equations find another, more preferable, solution:

- (a) if $k \leq 0$, the system undertakes a first-order phase transition. The new solution which develops at $T \geq T_M$, is characterized by a smaller system energy and a sudden increase of the Fermi level energy and the pairing gap (see, e.g., Fig. 2 in [6]);
- (b) if $k > 1$, the system undertakes a second-order phase transition. The new solution has smaller value of $|\delta\Delta_h + \delta\Delta_p|$. This phase transition is very similar to the superfluid – normal phase transition of the conventional BCS. But since the normal phase is not allowed in the MBCS (see [6]), the model predicts a phase transition of a superfluid state with a positive gap to another superfluid state with a negative gap.

We conclude that phase transitions of unknown types in the MBCS predictions at T_M are consequences of the thermal mechanism of pairing in this theory.

³ Independently from the physical content of the thermal gap in the MBCS, one finds from Eqs. (12)–(16) that $\delta\Delta_h \equiv -\delta\Delta_p$ for the conventional PFM and the cancellation between these two terms should be exact at any T . This does not happen in MBCS predictions because the MBCS theory violates Eqs. (12), (13), see above.

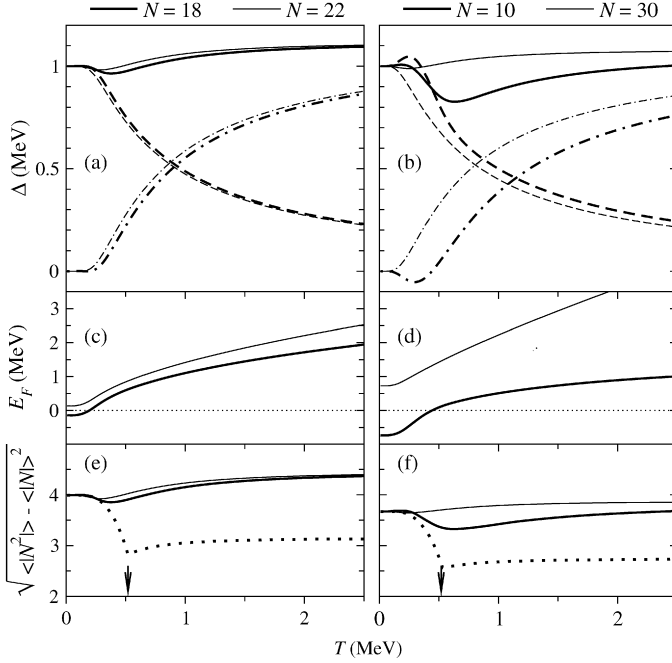


Fig. 6. MBCS predictions for (a), (b) the pairing gap, (c), (d) the energy of the Fermi level, and (e), (f) particle number fluctuations in the two-level model (the level degeneracy is 20). The number of particles N is 18 and 22 (left column) and 10 and 30 (right column): smaller N – thick lines, larger N – thin lines. Dashed and dot-dashed lines in (a), (b) present Δ_q and $(\delta\Delta_p + \delta\Delta_h)$ components of Δ , respectively. Dotted lines in (e), (f) plots particle number fluctuations in the conventional BCS. The conventional critical temperature T_c is shown by the vertical arrow.

A two-level model is another widely used model for testing the pairing problem. It is the PFM with $\Omega = 2$ and a degeneracy K for each level. The systems with a number of particles $N = K - k$ and $N = K + k$ (k is an integer value smaller than K) are particle/hole mirror systems and should have exactly the same solutions. Figure 6 presents the MBCS predictions for such mirror systems in calculations with parameters: $K = 20$, $\varepsilon_{\pm 1} = \pm 0.5$ MeV, and $\Delta_{T=0} = 1$ MeV. The calculations are performed for $k = \pm 2$ (left column) and $k = \pm 10$ (right column). The results for $k < 0$ and $k > 0$ are plotted by thick and thin lines, respectively.

The MBCS pairing gap is presented in Fig. 6(a), (b) by solid lines while its Δ_q and $(\delta\Delta_p + \delta\Delta_h)$ components are plotted by dashed and dot-dashed lines, respectively. The equivalence of the mirror systems in Fig. 6 is broken by the MBCS at finite temperatures. Disagreement becomes more sizable as k increases. The MBCS gap Δ is almost constant in these examples. Its thermal constituent $(\delta\Delta_p + \delta\Delta_h)$ behaves differently from what has been detected in Fig. 5 where this sum (the difference between thick and thin lines in Fig. 5) remains very small up to high temperatures. When the Fermi level is above ε_1 in the two-level model, there is no cancellation between $\delta\Delta_p$ and $\delta\Delta_h$ and both levels give positive contribution. The temperature dependence of the Fermi level energy is shown in Fig. 6(c), (d). Remember, thick and thin lines in Fig. 6(c), (d), representing mirror systems, should be symmetric against $E_F = 0$ (dotted-line).

The pairing induced by heating in systems with finite number of particles is discussed in the literature (see, e.g., Refs. [7–9]). However, this phenomenon is revealed by methods which exactly fix the number of particles in a finite system. The fixed number of particles is neces-

sary to take properly into account strong fluctuations of the order parameter (the pairing gap in the present case) which are important in systems with small number of particles. That is why the pairing correlations at finite temperature are considered in [7–9] in the canonical ensemble. The MBCS method conserves the particle number only on average like the conventional BCS method and the particle number fluctuations $\sqrt{\langle |N^2| \rangle - \langle |N| \rangle^2}$ is its inherent feature. Fig. 6(e), (f) presents this quantity for the two-level model. At the $T > T_c$ these fluctuations in the MBCS are even larger than in the conventional BCS. In our opinion, the only origin of temperature-induced pairing in the MBCS is the inconsistency in writing down the method equations (see Section 2).

6. Thermodynamic consistency of the MBCS theory

We now investigate the thermodynamic consistency of the MBCS observables by considering the system entropy. Different entropy-like quantities in nuclear physics: the thermodynamical entropy

$$S_{\text{th}} = \int_0^T \frac{1}{\tau} \cdot \frac{\partial E_{\text{tot}}}{\partial \tau} d\tau, \quad (17)$$

the single particle entropy (also referred to as the quasiparticle entropy in [10])

$$S_{\text{sp}} = - \sum_j (2j + 1) [n_j \ln n_j + (1 - n_j) \ln(1 - n_j)], \quad (18)$$

and the information entropy have been studied in [11,12]. It has been established that all of them “coincide for strong enough interaction . . . in the presence of a mean field” [12].

Fig. 7(a) presents the quantities $S_{\text{th}}^{\text{BCS}}$ and $S_{\text{sp}}^{\text{BCS}}$ (squares and crosses, respectively) for the $N = \Omega = 10$ PFM within the conventional BCS. It is not possible to visually distinguish between

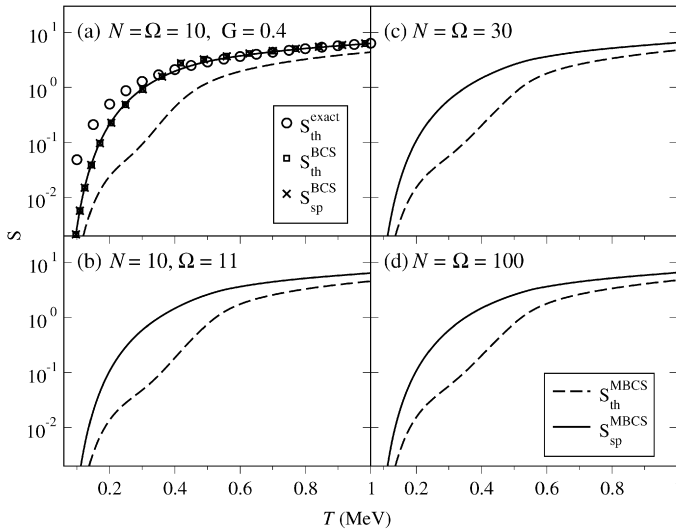


Fig. 7. MBCS predictions for the thermodynamical entropy S_{th} , Eq. (17), and the single particle entropy S_{sp} , Eq. (18) in different light and heavy, symmetric and asymmetric PFM systems. Note the logarithmic y scale.

them. The same is true for other PFM systems being considered and also in the case of a more realistic calculation in ^{120}Sn [5].

The quantities $S_{\text{th}}^{\text{MBCS}}$ and $S_{\text{sp}}^{\text{MBCS}}$ predicted by the MBCS model are plotted in Fig. 7 by dashed and solid lines, respectively. In this figure, we present different light and heavy, symmetric and asymmetric PFM systems. But in fact, the results do not depend on the number of particles N and levels Ω in the investigated temperature range. Thus, the $N = \Omega = 10$ PFM system may be considered as a typical example. Notice that $S_{\text{th}}^{\text{MBCS}}$ and $S_{\text{sp}}^{\text{MBCS}}$ are very different from each other up to an order of magnitude.

For the $N = \Omega = 10$ PFM system, the exact solution is available [13]. The system entropy $S_{\text{th}}^{\text{exact}}$ from this solution is plotted by circles in Fig. 7(a). One finds for $T > 100$ keV:

$$S_{\text{th}}^{\text{exact}} \approx S_{\text{th}}^{\text{BCS}} \cong S_{\text{sp}}^{\text{BCS}} \approx S_{\text{sp}}^{\text{MBCS}} \gg S_{\text{th}}^{\text{MBCS}}. \quad (19)$$

In passing we note that the quantities $S_{\text{th}}^{\text{MBCS}}$ and $S_{\text{sp}}^{\text{MBCS}}$ are compared to $S_{\text{sp}}^{\text{exact}}$ in Refs. [3, 10]. Unfortunately, the way $S_{\text{sp}}^{\text{exact}}$ is calculated produces the results which conflict with the third law of thermodynamics⁴ and, accordingly, wrong.⁵

We conclude that the system energy E_{tot} which enters Eq. (17) and the system entropy Eq. (18) are thermodynamically inconsistent quantities in the MBCS model. In another words, the MBCS expressions for the system energy (e.g., in the form of Eq. (25) in [3]) and entropy conflict to each other from the point of view of thermodynamics.

7. Conclusions

In this article we have investigated the validity of the MBCS model. The model performance is examined within the PFM to determine possible ranges of its applicability.

We confirm that there exists a single example of the PFM (with the number of levels Ω equal to the number of particles N plus one) in which the MBCS produces the thermal behavior of the pairing gap similar to the one of a macroscopic theory up to rather high temperatures. On the other hand, we demonstrate that in all other examples of the PFM with $\Omega \neq N$ the theory predicts phase transitions of unknown types at a much lower temperature.

The conventional PFM with $\Omega = N$ possesses internal particle–hole symmetry. Thus, some quantities in the model are known exactly. We have tested the MBCS predictions for these quantities and find significant deviations starting from very low temperatures.

A particular prediction of the MBCS is that heating generates a thermal constituent of the pairing gap in contrast to the generally accepted picture of the pairing phenomenon in nuclei to result from specific particle–particle interaction. We point out that this constituent of the MBCS pairing gap is responsible for phase transitions of unknown types. It also leads to a strong sensitivity of the theory predictions to tiny details of single particle spectra and is therefore unphysical. Finally, we point out that the MBCS is a thermodynamically inconsistent theory.

⁴ "... at absolute zero, any part of the body must be in a definite quantum state – namely the ground state ... the entropy of the body – the logarithm of its statistical weight – is equal to zero" (§23, p. 66 in [14]).

⁵ The author of [3,10] confused interacting particles (which have occupation probabilities for holes $f_h < 1$ and particles $f_p > 0$ at $T = 0$) and noninteracting "quasiparticles" (with occupation probabilities $n_{h(p)} \equiv 0$ at $T = 0$). Particle/hole levels are not eigen-states of the pairing Hamiltonian, their occupation numbers do not obey Fermi–Dirac distribution and because of that, they cannot be used in Eq. (18) which represents the free Fermi-gas combinatorics.

Acknowledgements

We thank P. von Neumann-Cosel for a critical reading of the manuscript and useful suggestions. The work was partially supported by the Deutsche Forschungsgemeinschaft (SFB 634).

References

- [1] N.D. Dang, V. Zelevinsky, *Phys. Rev. C* 64 (2001) 064319.
- [2] N.D. Dang, A. Arima, *Phys. Rev. C* 67 (2003) 014304.
- [3] N.D. Dang, *Nucl. Phys. A* 784 (2007) 147.
- [4] N.D. Dang, A. Arima, *Phys. Rev. C* 74 (2006) 059801.
- [5] V.Yu. Ponomarev, A.I. Vdovin, *Phys. Rev. C* 74 (2006) 059802.
- [6] V.Yu. Ponomarev, A.I. Vdovin, *Phys. Rev. C* 72 (2005) 034309.
- [7] L.G. Moretto, *Phys. Lett. B* 40 (1972) 1.
- [8] S. Frauendorf, N.K. Kuzmenko, V.M. Mikhajlov, J.A. Sheikh, *Phys. Rev. B* 68 (2003) 024518.
- [9] J.A. Sheikh, R. Palit, S. Frauendorf, *Phys. Rev. C* 72 (2005) 041301(R).
- [10] N.D. Dang, *Phys. Rev. C* 76 (2007) 064320.
- [11] V. Zelevinsky, B.A. Brown, N. Frazier, M. Horoi, *Phys. Rep.* 276 (1996) 85.
- [12] V.K. Kota, R. Sahu, *Phys. Rev. E* 66 (2002) 037103.
- [13] A. Storozhenko, P. Schuck, J. Dukelsky, G. Röpke, A. Vdovin, *Ann. Phys.* 307 (2003) 308.
- [14] L.D. Landau, E.M. Lifshitz, *Statistical Physics*, Pergamon Press, London–Paris, 1958.